

Reliable calculations of level densities using statistical spectroscopy.

Jameel-Un Nabi¹, Calvin W. Johnson¹ and W. Erich Ormand²

¹*Department of Physics and Astronomy*

Louisiana State University, Baton Rouge, LA 70803-4001

²*Lawrence Livermore National Laboratory*

P.O. Box 808, Mail Stop L-414

Livermore, CA 94551

Abstract

Nucleosynthesis calculations require nuclear level densities for hundreds or even thousands of nuclides. Ideally one would like to constrain these level densities by microscopically motivated yet computationally cheap models. A statistical approach suggests that low moments of the Hamiltonian might be sufficient. Recently Zuker proposed a simple combinatoric formula for level densities based upon the binomial distribution. We rigorously test the binomial formula against full scale shell-model diagonalization calculations for selected *sd*- and *pf*-shell nuclides and also against Monte Carlo path integration calculations. We find that the fourth moment is as important as the third moment to a good description of the level density, as well as partitioning of the model space into subspaces.

I. INTRODUCTION

Nuclear level densities are important for the theoretical estimates of nuclear reaction rates in nucleosynthesis. The neutron-capture cross sections are approximately proportional to the corresponding level densities around the nuclear resonance region. The competition between neutron-capture and β decay determines the fate of the *s*- and *r*-processes. The abundance of *s*-process nuclei with nonmagic neutron number is inversely proportional to the neutron-capture cross section [1], i.e., proportional to the level density. The waiting points of the *r*-process are determined by the balance between the rates of neutron-capture and of photoejection of a neutron.

Reliable estimates of nuclear abundances require accurate level densities. Authors like Gilbert and Cameron [2] gave uncertainties beyond a factor of 10 in their early calculations and uncertainties of about a factor of 8 and 5 are present in calculations of [3] and [4], respectively. What is desired is a reliability within a factor of two.

At low excitation energies (up to 5 MeV), level densities are usually extracted experimentally via direct counting from neutron/proton resonance data [5]. For intermediate energies (between 5 and 15 MeV) they are extracted from charged particles spectra [6,7] while for still higher energies the level densities are determined using the Ericson fluctuation analysis [6]. Recently, the Oslo group has reported on a new method to extract level density from primary γ -ray spectra without the assumption of any model [8].

Such experimental measurements are very labor intensive, and reaction network calculations require hundreds or thousands of cross sections, sometimes for unstable nuclides. Therefore one turns to theoretical models for help.

Most conventional calculations of the nuclear level density are based on the Fermi gas model. The most widely used description of the nuclear level density is the Bethe formula, based on a gas of free nucleon [9]. This parameterization works well for the level densities of many nuclides at low energies and in the neutron energy region [10] especially when one uses the modified “backshifted Bethe formula” [11,12]. Unfortunately the fitted single-

particle level density parameter and the backshift parameter are nucleus-dependent and are not derived theoretically. Rauscher and collaborators presented a global parametrization of nuclear level densities within the back-shifted Fermi-gas formalism [13]. They employed an energy-dependent level density parameter and a backshift parameter to attain an improved fit of level densities at neutron-separation energies. Despite all this, the fact remains that the input parameters are just that: empirically fitted parameters.

Can one look to theory for help? The interacting shell model and other microscopic models accurately describe spectra and transition for a broad range of nuclides. On the other hand, “traditional” shell-model codes diagonalize the Hamiltonian in a large-dimensioned basis of occupation-state wavefunctions but use the Lanczos algorithm to extract only a handful low-lying states. The level density requires all eigenstates and thus complete diagonalization, a computationally forbidding requirement.

An alternative to diagonalization is the Monte Carlo path-integral technique [14], which is well suited to thermal observables [15–17]. Nakada and Alhassid [16] extracted both the single-particle level density parameter and the backshift parameter from the microscopic Monte Carlo densities by fitting them to the backshifted Bethe formula and also found some shell effects in their systematics. Recent developments include the particle number reprojection method [18], which can calculate level densities of odd-even and odd-odd nuclei despite a sign problem introduced by the projection of an odd number of particles. Path-integral methods are limited, however, to interactions that are free of the ‘sign problem.’ Therefore we consider alternatives.

One possibility is nuclear statistical spectroscopy [19,20], which argues that many nuclear properties are controlled by low-lowering moments of the Hamiltonian. Given a set of one- and two-body interaction matrix elements (the same input for a shell-model diagonalization or path-integral calculation) one can readily find in the literature straightforward formulae for first through fourth moments [19–21]. One early result of statistical spectroscopy was that for a finite model space, the total level density tends to be Gaussian [22]. Of course this means the model ignores intruders at high excitation energy, but it also suggests that

the level density even at low energy is governed by the width, or second moment, of the Hamiltonian. Grimes and collaborators included 4th moment [23,24] in order to improve the description of the level densities. Recently Zuker suggested a modified approach [25]. He argued that a binomial distribution rather than Gaussian arises most naturally from combinatorial arguments. In the limit of an infinite number of states the binomial becomes a Gaussian; but for a finite model space the differences are nontrivial as we shall discuss.

This paper discusses in detail the implementation of a novel treatment of level density descriptions using statistical models introduced recently by Johnson, Nabi and Ormand [26]. Here we compare these models against a number of nuclei whose level densities can be fully computed by diagonalization of a two-body Hamiltonian in the *sd*- or *pf*-shells. We also compare against Monte Carlo path integration calculations for nuclides where direct diagonalization is not possible. We find that in most cases it is the *fourth* moment which distinguishes among the exact, Gaussian, and binomial level densities, although we find cases in which the 3rd moment is important.

Section 2 presents the formalism of our calculations. Section 3 shows some comparison of the Gaussian and binomial level densities with the microscopic level densities. In section 4 we present a curious finding, that there is a relation between the fourth moment of individual particle configurations and collectivity, which suggests a possible way to use statistical spectroscopy to model the low-lying, non-statistical collective structure of the nuclides. Here we partition the model space into subspaces, use the binomial distribution to construct partial level densities and finally sum them to get the total level density. These improved models depict a more realistic picture of the microscopic level densities. We conclude and summarize in Section 5.

II. FORMALISM

Nuclear statistical spectroscopy [19,20], championed by French and collaborators, is built upon moments of the nuclear Hamiltonian \hat{H} in a finite many-body space. The first moment

or centroid is

$$\mu_1 = \bar{H} \equiv \langle \hat{H} \rangle; \quad (1)$$

all other moments are central moments:

$$\mu_n \equiv \langle (\hat{H} - \bar{H})^n \rangle. \quad (2)$$

As one computes higher and higher moments, one naturally regains more and more information about \hat{H} . But higher moments are difficult to calculate. An alternative is to partition the model space into subspaces \mathcal{S}_α , using projection operators $P_\alpha = \sum_{a \in \alpha} |a\rangle \langle a|$. We call

$$\mu_n(\alpha) \equiv \langle P_\alpha (\hat{H} - \bar{H})^n \rangle \quad (3)$$

a *configuration* moment, and general formulae can be found in the literature for configuration moments up to $n = 4$ [19,21]. The total central moments can be easily found by summing over the configuration moments.

The density of states can be formally written as

$$\rho(E) = \text{tr} \delta(E - \hat{H}). \quad (4)$$

One can also introduce *configuration* densities (sometimes called *partial* densities)

$$\rho_\alpha(E) = \text{tr} P_\alpha \delta(E - \hat{H}), \quad (5)$$

to which we will return later. If the *many-body* matrix elements of \hat{H} are randomly distributed (specifically, if they belong to a Gaussian Orthogonal Ensemble) then the density of states of \hat{H} follow a semi-circle distribution. If \hat{H} however is a two-body operator then the many-body matrix elements are correlated and the density of states is Gaussian, or at least nearly so [22].

The Gaussian and semi-circle distributions differ in their higher moments. Let the *scaled* moments be defined by

$$m_n \equiv \mu_n / (\mu_2)^{n/2}, \quad (n > 2), \quad (6)$$

as the width μ_2 provides a natural energy scale. The scaled fourth moment m_4 is 3 for a Gaussian but is 2 for the semi-circle distribution. A Gaussian is reasonable good starting point as it is already close to the actual level density. A common generalization is to expand in a Gram-Charlier series using Hermite polynomials [20]; this unfortunately can lead to negative level densities. Another generalization is to extend the Gaussian to a function of the form $\exp(-\alpha E^2 - \beta E^3 - \gamma E^4 \dots)$ [27,24] but the relation between parameters α, β, γ and the moments is not amenable to a simple analytic formula.

Recently Zuker gave a combinatorial argument that one should use a binomial distribution rather than Gaussian to approximate level densities [25]. We only summarize his approach here. Consider the binomial expansion

$$(1 + \lambda)^N = \sum_{k=0}^N \lambda^k \cdot \binom{N}{k} \quad (7)$$

Now interpret this binomial expansion as a distribution of levels, specifically, that $\lambda^k \binom{N}{k}$ is the number of states at excitation energy $E_x = \epsilon k$, ϵ being an overall energy scale. Because we can write $\binom{N}{k}$ with gamma functions, one can easily generalize to the continuous case,

$$\rho(E_x) = \lambda^{E_x/\epsilon} \frac{\Gamma(E_{max}/\epsilon + 1)}{\Gamma(E_x/\epsilon + 1)\Gamma((E_{max} - E_x)/\epsilon + 1)} \quad (8)$$

where $E_{max} = \epsilon N$. Although we began with N as an integer, it no longer has to be.

The binomial distribution has several advantages. In the limit $\lambda = 1, N \rightarrow \infty$ one regains the Gaussian. For $\lambda \neq 1$ the distribution is asymmetric, because of a non-zero third moment; Zuker makes a combinatorial argument that the third moment can be as significant as the second moment. Finally, unlike most generalizations to the Gaussian, such as adding a γE^4 term to the argument of the exponential, one can easily compute the moments of the binomial. The total number of levels, which is in effect the ‘zeroth’ moment, is

$$d = (1 + \lambda)^N, \quad (9)$$

while the centroid and width are given by

$$\mu_1 = \frac{N\epsilon\lambda}{1+\lambda} \quad (10)$$

$$\mu_2 = \frac{N\epsilon^2\lambda}{(1+\lambda)^2} \quad (11)$$

and the *scaled* third and fourth moments are

$$m_3 = \frac{1-\lambda}{\sqrt{N\lambda}}, \quad (12)$$

$$m_4 = 3 - \frac{4-\lambda}{N} + \frac{1}{N\lambda}. \quad (13)$$

Ref [25] does not give the fourth central moment. For Gaussians ($N \rightarrow \infty$) $m_4 = 3$. For most binomials and for shell model diagonalization, the scaled fourth moment is less than 3, a typical value being around 2.8. (Note that the above moments are exact for discrete distributions but are only approximate for the continuous distributions, due to errors in integration. For large N , however, they are very good approximations.)

Using Stirling's approximation, and a few others, Zuker arrives at

$$\rho(E_x) \approx \sqrt{\frac{8}{N\pi}} \exp \left(-(N-1) \left(\frac{E_x}{E_{max}} \ln \frac{E_x}{E_{max}} + \frac{E_{max} - E_x}{E_{max}} \ln \frac{E_{max} - E_x}{E_{max}} \right) + N \frac{E_x}{E_{max}} \ln \lambda \right). \quad (14)$$

The key parameters of the binomial are the order N and the asymmetry parameter λ . If $\lambda = 1$ then the binomial is *symmetric* and has $m_3 = 0$; if $\lambda \neq 1$ then the binomial is *asymmetric* or skewed. The skewness can be positive ($m_3 > 0, 0 < \lambda < 1$), or negative ($m_3 < 0, \lambda > 1$). Zuker suggested that the order of the binomial, N , be fixed by the dimension of the model space. In that case N and λ are fixed by solving eqns. (9) and (12) simultaneously. This we consider to be the 'standard' binomial. We note, however, that one could instead fix the order N by the fourth moment, and solve (12) and (13) simultaneously instead, afterwards multiplying the entire binomial distribution by a constant so as to get the correct total number of levels. This we refer to as the *fourth-moment scaled* (FMS) binomial. After N and λ are determined, the centroid and width simply fix the absolute scale of the distribution.

The central question of this paper is which distribution—Gaussian, binomial, FMS binomial, or some (other) improved model—best describes microscopic level densities? We use the low moments, in particular the third and fourth moment, to characterize our results.

III. COMPARISON OF LEVEL DENSITIES WITHOUT PARTITIONS

To test binomials as candidates for modeling level densities, we compare against exact shell model calculations. (All the densities shown in our figures are in fact *state* density, which includes $2J + 1$ degeneracies. Strictly speaking, the *level density* ignores $2J + 1$ degeneracies, but the literature is often cavalier with this distinction). In this section we do not partition the model space into configuration subspaces, which will be considered in the next section.

We considered full $0\hbar\omega$ *sd*- and *pf*-shell calculations, and focused on several nuclides that could be completely diagonalized using the OXBASH shell-model code [28]. In the *sd*-shell we used the Wildenthal USD interaction [29] and performed exact shell model calculations for many nuclides covering the entire range. In the *pf*-shell we used the Brown-Richter interaction [30] and computed $^{44,45}\text{Ti}$. For still larger dimensions, we turned to Monte Carlo path integration calculations [14–17]. To avoid the well-known sign problem [14] we fitted a schematic multipole-multipole interaction to the $T = 1$ matrix elements of the Brown-Richter interaction [30]. For all of these calculations we computed the exact spectroscopic moments, using the same single-particle energies and two-body interaction matrix elements were used by OXBASH. As far as we know this is the first time the exact formulas of [21] for third and fourth moments have been computed for a general case [31].

We ask: Is there a significant difference between exact, Gaussian, and binomial level densities, and is the difference driven by third or fourth moments? First the moments. Table 1 shows the scaled third and fourth moments for the exact distributions (the moments from exact shell model eigenvalues and those calculated using [21,31] should and do agree) as well as fourth moment for ‘standard’ binomials for some selected *sd*- and *pf*-shell nuclides.

(Remember that the third and fourth moments for a Gaussian are 0 and 3, respectively.) The third moment is generally small, except for the case of ^{20}F , ^{24}Ne , ^{28}Na and ^{36}Ar in the sd -shell and ^{54}Mn and ^{54}Fe in the pf -shell; we found a strong correlation between nontrivial m_3 and $T_z \neq 0$. Because the standard binomial parameters N and λ are found by solving Eqn. (9) and (12) (that is, constrained by the total number of levels and the third moment), the fourth moment, m_4 , is *not* constrained. We see from Table 1 that on the average, the (standard) binomials tend to overestimate the scaled fourth moment, m_4 . We further note that whenever the magnitude of the scaled third moment is ≥ 0.05 (which we regard as a significant value), the difference in the exact and binomial scaled fourth moment is considerable, albeit less so for the pf -shell nuclides.

Fig. 1 shows two sample sd - and two pf -shell nuclides. The histograms are the result of direct diagonalization. The figure shows the exact spectrum, the Gaussian and the two binomials (symmetric and asymmetric). For the symmetric case we forced the asymmetry parameter λ to be 1 (the fourth moment did not change significantly). Because the symmetric and asymmetric binomial distributions are very similar for all these cases, we conclude that it is the fourth moment rather than the third moment that drives the difference. For ^{45}Ti , in fact the symmetric and asymmetric binomials are indistinguishable. We remind the reader that our goal is a factor of 2 accuracy in modeling the level density.

But what if the scaled third moment is significantly different from zero (i.e. if the absolute value is ≥ 0.05)? Intuition dictates that the third moment should play a role for such cases. Figure 2 shows the case for nuclides with large asymmetry. Again we chose two sd - and two pf -shell nuclides. The open circles in Fig. 2 show the Monte Carlo shell model calculations along with the uncertainties. Here there is a clear difference between the symmetric and asymmetric binomials as expected. For these cases there also exist a large discrepancy between the binomial and exact m_4 . We therefore also plot the FMS (fourth-moment-scaled) binomial, which has the correct m_4 . The FMS binomial has clearly a better behavior especially for the pf -shell nuclides. Unfortunately the scaling also leads to a cut-off (unlike a Gaussian, the binomial has sharp cutoffs and infinite slope at $E_x = 0, E_{max}$) which

is too high for the case of ^{24}Ne .

The preliminary lessons that we learn: binomial distribution *do* model shell-model level densities better than Gaussians, but in many cases it is the fourth moment rather than the third that leads to a discrepancy. Nuclides with $T_3 \neq 0$ have larger asymmetries, however, and must be accounted for. A scaled third moment of about ± 0.05 is non-negligible. While an obvious solution is to adjust the binomial to reproduce the exact fourth moment, the binomial's abrupt cut-off in certain cases, leads us to generalize our approach to a partitioned model space, described in the next section.

IV. SUM OF PARTITIONED BINOMIAL (SUPARB) LEVEL DENSITIES

To improve our results we partition the model space into configuration subspaces. One expects partitioned models to better approximate the higher moments [32,33] (for example, Pluhar and Weidenmüller [32] had a sum of distorted semi-circles and got much better modeling than a single semi-circle). We also saw in the previous section that the FMS binomial gets the fourth moment correct but stops abruptly. Partitioning of the model space into subspaces solves this problem.

We partitioned the model space by single-particle configurations, such as $(1s_{1/2})^2(0d_{3/2})^1(0d_{5/2})^3$, for the very simple reason that analytic formulas exist for the associated configuration moments. Other possibilities would be to partition by J, T or by $SU(3)$; unfortunately no analytic formulas exist for these partitions. We did consider J, T partitions, computing the moments by hand (the OXBASH shell model code projects the Hamiltonian onto J, T partitions) but we did not find significant advantage. $SU(3)$ would be an attractive partitioning, as it would naturally build in quadrupole collectivity, but even by hand this is difficult for a general two-body interaction. Experts should note that protons and neutrons orbits were considered distinct, which would allow us to easily project exact isospin.

To compute the level densities, we take the following steps: (1) We compute the config-

uration moments up to 4th order. (2) We model the partial density for each configuration as a binomial (either standard or FMS). The binomial parameters N_α and λ_α , as well as the overall energy scale and centroid, are fitted to the configuration moments for the α^{th} subspace. The binomial then gives a partial density. (3) The partial densities are summed to yield the total level densities. Because of these ingredients, we will refer to our approach as SUPARB (SUM of PARtitioned Binomials) level densities. If we model the partial densities for the configurations as a FMS binomial, i.e., if we fix the order N_α by the fourth moment, and solve (12) and (13) simultaneously for each configuration, we call the resulting sum as SUPARB-FMS.

Fig. 3 models the state densities for four *sd*-shell nuclides, ^{23}Ne , ^{24}Mg , ^{32}P , and ^{32}S . Here we plot the SUPARB and SUPARB-FMS state densities against the exact ones. We see that not only the SUPARB-FMS densities model the exact state densities some what better, some structure in the low-lying states is also revealed. Such structure cannot be described by simple models such as either a Gaussian or a binomial. The structure is particularly very profound for the low-lying states of ^{24}Mg and ^{32}S . There were however cases where no appreciable difference between the SUPARB and SUPARB-FMS state densities was found. Fig. 4 shows four such cases: ^{22}Ne , $^{22,24}\text{Na}$, and ^{23}Mg . We see that the comparison is again very good (within a factor of 2) and that there is no appreciable difference between the SUPARB and SUPARB-FMS state densities.

The computation time of moments, μ_n , scales as (number of partitions)(number of j-orbits) 2n . That is, calculation of fourth moments requires much more CPU time as compared to the third one. SUPARB-FMS is sometime a clearly superior model but there are also cases where SUPARB alone gives equally good results. Two important questions then arise: (1) Is it possible to determine the cases where SUPARB state densities are sufficient, merely by looking at the configuration third moments in order to save time? and (2) What are the reasons behind when SUPARB-FMS gives better results? When do we see the low-lying structure in SUPARB-FMS?

The answers to these questions do not seem to be simple. There are clues, however, to

the choice between the two SUPARB densities. One clues lies in the spread of the scaled third configuration moments. If there is a spread of these moments both above 0.05 and below -0.05, SUPARB-FMS is likely to produce better results. Fig. 5 shows the spreads in the scaled third configuration moments $m_3(\alpha)$, where α labels the configuration, for some selected nuclides from Figs. 3 and 4. The ordinate is the associated configuration centroid h_α which indicates the average excitation energy of states in the subspace α . (We have neglected a few of the configuration third moments in all the four cases with values much less than -0.05.) The bulk of the $m_3(\alpha)$ lie in the range $-0.2 \leq m_3 \leq 0.2$. Any $m_3(\alpha)$ which falls outside the rectangle is to be taken as significant. What we see is that for the graphs in the left column there is a spread of m_3 around the rectangle. For the right column we do not see any $m_3 > 0.05$. And we see that for these two cases (^{22}Ne and ^{24}Na), standard SUPARB densities do equally well (see Fig. 3). So for these cases there is no special need for computation of the scaled fourth moments (similar is the case for ^{23}Mg and ^{22}Na).

There can be a problem for high positive values of m_3 , $\lambda \rightarrow 0$, and the binomial $m_3 \rightarrow \frac{1}{\sqrt{\ln d}}$. So, for example, if the dimension $d = 500$, by Equation (12) the maximum m_3 allowed by the standard binomial is 0.16. For any value of exact $m_3 > 0.16$ the standard binomial fails. Frequently we found large values of m_3 for configurations even of small dimension. Fortunately, for fourth-moment-scaled (FMS) binomials, this is not as limiting (we fix the order N_α by the fourth moment, solve (12) and (13) simultaneously, and afterwards multiply the entire binomial distribution by a constant so as to get the correct total number of levels) and the technique can be applied to all cases.

Regarding the answer to the second question, the reply lies partly in what we already described previously. Empirically we find that a spread of exact $m_3(\alpha)$ around ± 0.05 , is likely to reveal some structure. Again if we look at Fig. 5 we do see that for ^{23}Ne and ^{32}P there is a spread of m_3 above and below the rectangle; simultaneously, Fig. 4 shows nontrivial structure at very low excitation energy for these nuclides. The same pattern occurs for ^{24}Mg and ^{32}S , suggesting that the two events are correlated.

Yet another clue lies in the $m_4(\alpha)$ shown in Fig. 6. We note that for cases where SUPARB-

FMS densities reveal some structure, the standard binomials systematically overestimate the configuration scaled fourth moments. One clearly sees that for ^{24}Mg and ^{32}S , the (standard) binomial $m_4(\alpha)$ are biased high compared to their exact values. On the other hand, for ^{22}Na and ^{23}Mg , relatively structureless at low excitation energy, the binomial $m_4(\alpha)$'s are not biased relative to their exact values but fall both high and low symmetrically.

Let us summarize what we have said so far for these improved statistical models of level densities. SUPARB-FMS density can be a better choice, not only in modeling the secular behavior (within a factor of two) but also reveals some structure in certain cases, specially for the interesting low-lying region. It however, requires a larger CPU time which can be a big problem when modeling thousands of cases. SUPARB density is still better compared to a single binomial density but for large, positive m_3 (which is very common for partitioned subspaces) they are constrained by the dimension of the configurations.

V. CONCLUSIONS

We have outlined a theoretical approach to level densities that is both microscopic in origin and also computationally tractable. We analyzed our results in terms of the third and fourth moments. For small asymmetries, the fourth moment dominates. For cases where the scaled third moment is significantly different from zero (with magnitude greater than 0.05) the binomials are characterized by both the third and fourth central moments. The FMS binomial gives the best description of the exact level densities, specially when the nuclides have a large scaled third moment. There is an improvement over the asymmetric standard binomial by as much as a factor of 2 in the modeling of the low-lying exact level densities. Our study also shows that the Gaussians continue to give a good estimate of the exact spectrum for the level densities (within a factor of 5) and this comes quite handy since they just require the centroid and width of the Hamiltonian as input parameters. They might be used for an initial estimate of level density and then the interesting cases can be followed by still refined models presented here.

Partitioning the space considerably improves the binomial approximation to the level densities. The SUPARB-FMS has some in-built structure and follows the trend of the exact level density specially in the collective regime. The degree of precision of the present approach will give astrophysical nucleosynthesis calculations a much better predictive power. Future application to higher shells will be hampered as much by our ignorance of the effective two-body interaction as anything else. SUPARB can also be easily generalized to the calculation of spin-cutoff factors, and we are planning to make application to nuclear heat capacities and estimate of contamination by spurious center-of-mass motion.

This work was performed under the auspices of the Louisiana Board of Regents, contract number LEQSF(1999-02)-RD-A-06; and under the auspices of the U.S. Department of Energy through the University of California, Lawrence Livermore National Laboratory, under contract No. W-7405-Eng-48.

REFERENCES

- [1] P. A. Seeger, W. A. Fowler, and D. D. Clayton, *Astrophys. J. Suppl.* **11**, 121 (1965).
- [2] A. Gilbert and A.G.W. Cameron, *Can. J. Phys.* **43**, 1446 (1965).
- [3] S.E. Woosley, W.A. Fowler, J.A. Holmes and B.A. Zimmerman, *At. Nucl. Data Tables* **22**, 371 (1978).
- [4] F.-K. Thielemann, M. Arnould and J.W. Truran, *Advances in Nuclear Astrophysics*, eds. E. Vangioni-Flam et. al. p.525.
- [5] W. Dil, W. Schantl, H. Vonach and M. Uhl, *Nucl. Phys. A* **217**, 269 (1973).
- [6] J.R. Huizenga, H.K. Vonach, A.A. Katsanos, A.J. Gorski and C.J. Stephan, *Phys. Rev.* **182**, 1149 (1969).
- [7] C.C. Lu, L.C. Vaz and J.R. Huizenga, *Nucl. Phys. A* **190**, 229 (1972).
- [8] A. Schiller, L. Bergholt, M. Guttormsen, E. Melby, J. Reststad and S. Seim, *Nucl. Instum. Methods A* **447**, 498 (2000).
- [9] H.A. Bethe, *Phys. Rev.* **50**, 332 (1936).
- [10] A. Bohr and B.R. Mottelson, *Nuclear Structure* vol. 1 (Benjamin, New York, 1969).
- [11] J.A. Holmes, S.E. Woosley, W.A. Fowler and B.A. Zimmerman, *Atom. Data, Nucl. Data Tables* **18**, 305 (1976).
- [12] J.J. Cowan, F.-K. Thielemann and J.W. Truran, *Phys. Rep.* **208**, 267 (1991).
- [13] T. Rauscher, F.-K. Thielemann and K.-L. Kratz, *Phys. Rev. C* **56**, 1613 (1997).
- [14] C.W. Johnson, S.E. Koonin, G.H. Lang and W.E. Ormand, *Phys. Rev. Lett/* **69**, 3157 (1992).
- [15] D.J. Dean, S.E. Koonin, K. Langanke, P.B. Radha and Y. Alhassid, *Phys. Rev. Lett.* **74**, 2909 (1995).

- [16] H. Nakada and Y. Alhassid, Phys. Lett. B **436**, 231 (1998).
- [17] J.A. White, S.E. Koonin and D.J. Dean, Phys. Rev. C **61**, 034303 (2000).
- [18] Y. Alhassid, S. Liu and H. Nakada, Phys. Rev. Lett. **83**, 4265 (1999).
- [19] J.B. French and K.F. Ratcliff, Phys. Rev. C **3**, 94 (1971).
- [20] S. S. M. Wong, *Nuclear Statistical Spectroscopy*, Oxford Press (New York, 1986).
- [21] S. Ayik and J.N. Ginocchio, Nucl. Phys. A **221**, 285 (1974).
- [22] K. K. Mon and J. B. French, Ann. Phys. **95**, 90 (1975).
- [23] S. M. Grimes, S. D. Bloom, R. F. Hausman, Jr. and B. J. Dalton, Phys. Rev. C **19**, 2378 (1979).
- [24] S. M. Grimes, S. D. Bloom, H. K. Vonach and R. F. Hausman, Jr., Phys. Rev. C **27**, 2893 (1983).
- [25] A. P. Zuker, Phys. Rev. C **64**, 021303 (2001).
- [26] C. W. Johnson, J.-U. Nabi and W. E. Ormand, submitted to Phys. Rev. Lett. (2001), LANL archive nucl-th/0105041.
- [27] F. S. Chang and A. Zuker, Nucl. Phys. A **198**, 417 (1972).
- [28] B. A. Brown, A. Etchegoyen, and W. D. M. Rae, OXBASH, the Oxford University-Buenos Aires-MSU shell model code, Michigan State University Cyclotron Laboratory Report No. 524 (1985).
- [29] B.H. Wildenthal, Prog. Part. Nucl. Phys. **11**, 5 (1984).
- [30] W. A. Richter, M. G. van der Merwe, R. E. Julies, and B. A. Brown, Nucl. Phys. **A523**, 325 (1991), Nucl. Phys. **A557**, 585 (1994).
- [31] J.-U. Nabi and C. W. Johnson, program CONMOM4, to be published.

[32] Z. Pluhar and H. A. Weidenmüller, *Phys. Rev. C* **38** (1988) 1046.

[33] V. K. B. Kota, D. Majumdar, *Nucl. Phys. A* **604**, 129 (1996).

Table (1): Scaled third and fourth moments. The exact fourth moments are compared with those of standard binomials.

Nuclides	m_3	m_4 (exact)	m_4 (standard binomial)	Nuclides	m_3	m_4 (exact)	m_4 (standard binomial)
^{20}F	0.12	2.60	2.86	^{32}Si	0.024	2.90	2.87
^{20}Ne	0.092	2.71	2.83	^{30}P	0.0053	2.79	2.89
^{24}Ne	0.10	2.80	2.92	^{32}P	-0.023	2.78	2.86
^{22}Na	0.036	2.81	2.87	^{32}S	-0.037	2.77	2.86
^{24}Na	0.057	2.78	2.90	^{30}Cl	0.054	2.76	2.90
^{26}Na	0.088	2.76	2.92	^{32}Cl	-0.021	2.84	2.86
^{28}Na	0.14	2.73	2.94	^{34}Cl	-0.073	2.88	2.82
^{23}Mg	0.035	2.80	2.88	^{36}Ar	-0.12	2.97	2.74
^{24}Mg	0.036	2.81	2.89	^{44}Ti	0.036	2.82	2.87
^{24}Al	0.058	2.83	2.90	^{45}Ti	-0.0026	2.89	2.87
^{26}Al	0.039	2.81	2.90	^{48}Cr	-0.071	2.96	2.89
^{28}Al	0.038	2.79	2.90	^{54}Mn	-0.11	2.96	2.91
^{30}Al	0.054	2.77	2.90	^{54}Fe	-0.11	2.93	2.91

FIGURES

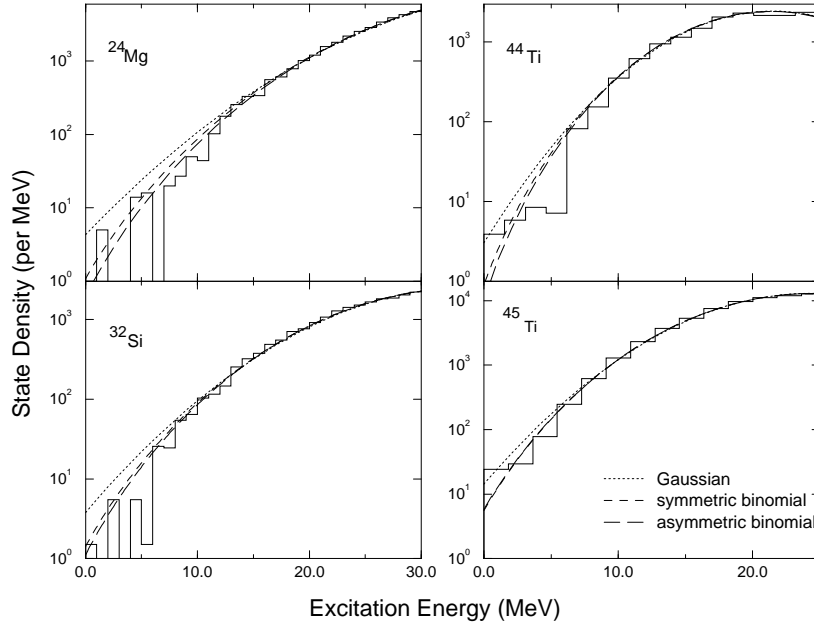


FIG. 1. Comparison of exact shell model state densities (histograms) against Gaussians and binomials for *sd*- and *pf*-shell nuclides.

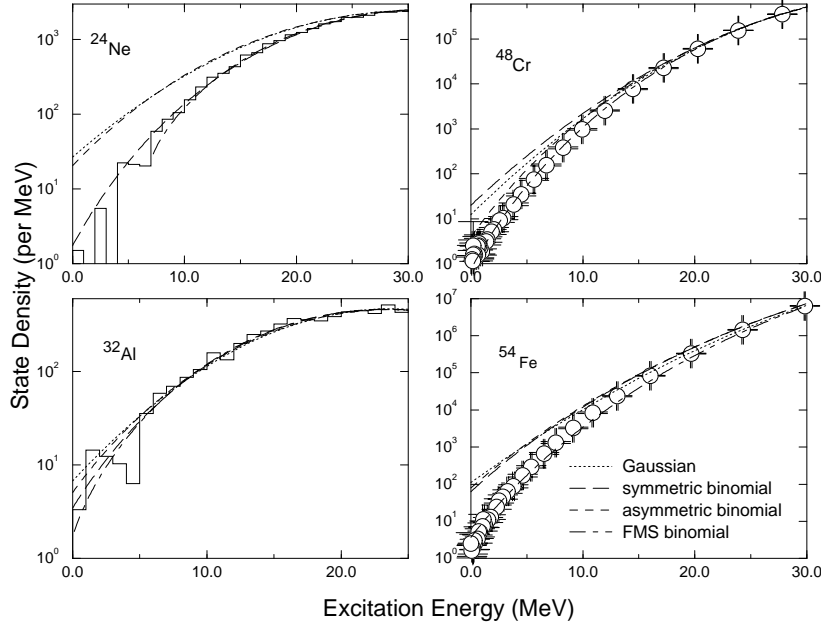


FIG. 2. Comparison of exact shell model state densities (histograms) against Gaussians and binomials for *sd*- and *pf*-shell nuclides. The circles represent the Monte Carlo path integration calculation in a full $0\hbar\omega$ basis along with the uncertainties. FMS = “fourth moment scaled” (see text).

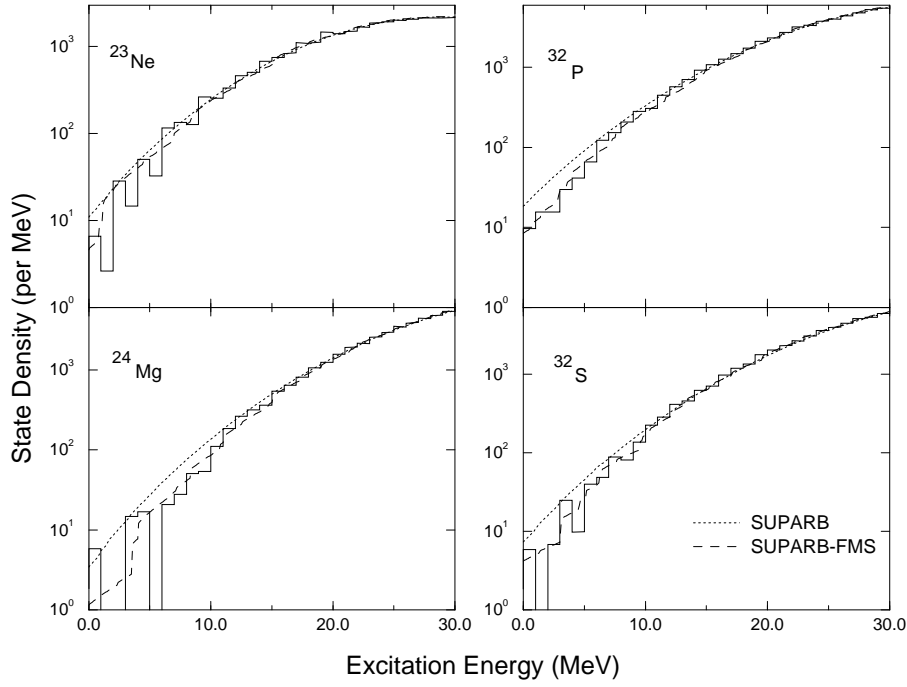


FIG. 3. Comparison of exact shell model state densities (histograms) against sum of partitioned binomial densities (SUPARB) and sum of partitioned binomial densities which are fourth moment scaled (SUPARB-FMS). Note the structure in the SUPARB-FMS densities.

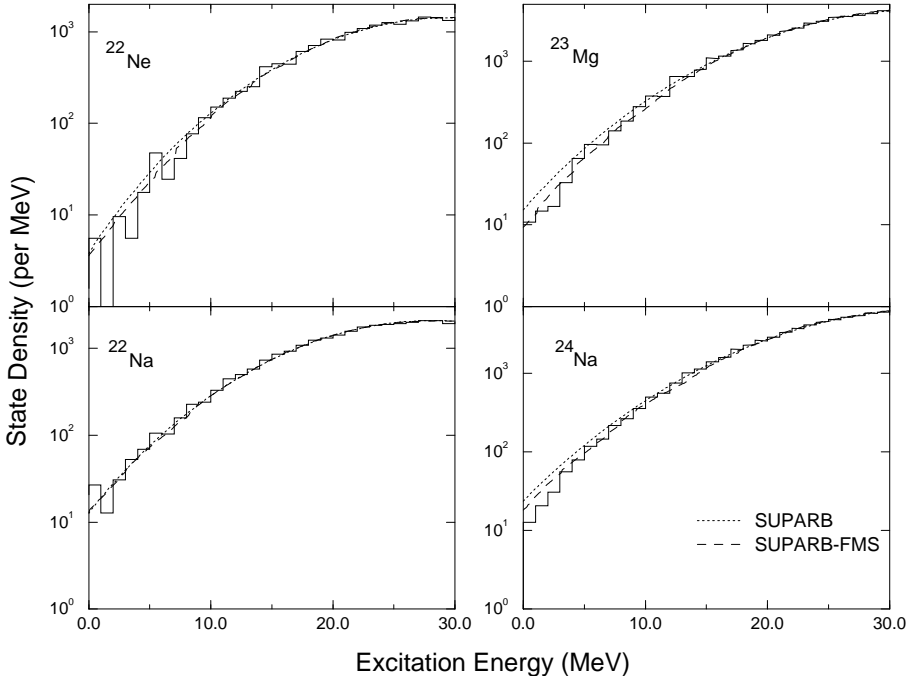


FIG. 4. Same as Fig. 3 but for four other *sd*-shell nuclides. Here there is little distinction between standard and fourth-moment-scaled binomials.

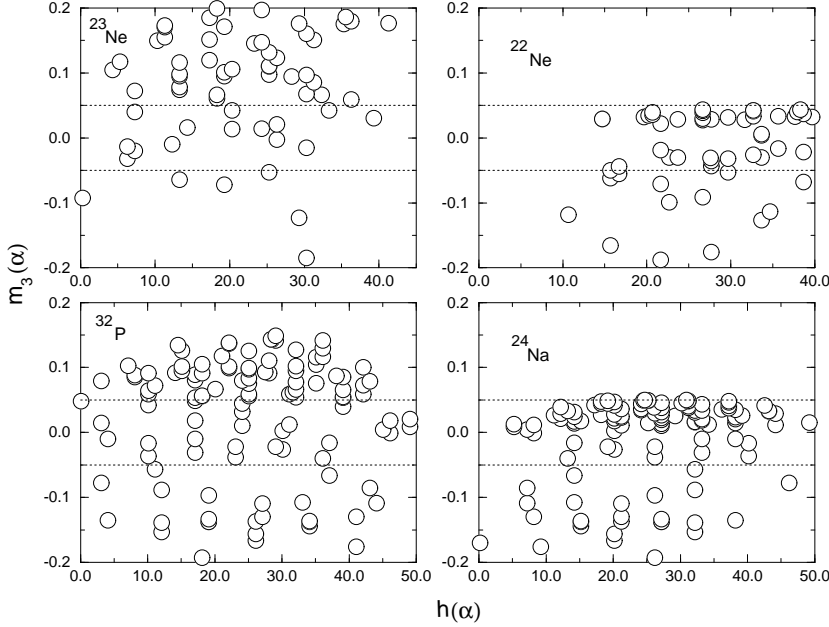


FIG. 5. Spread of configuration scaled third moments $m_3(\alpha)$ as a function of configuration centroids $h(\alpha)$ (relative to the ground state energy). Any value of $m_3(\alpha)$ outside the dotted rectangle represents a significantly high value.

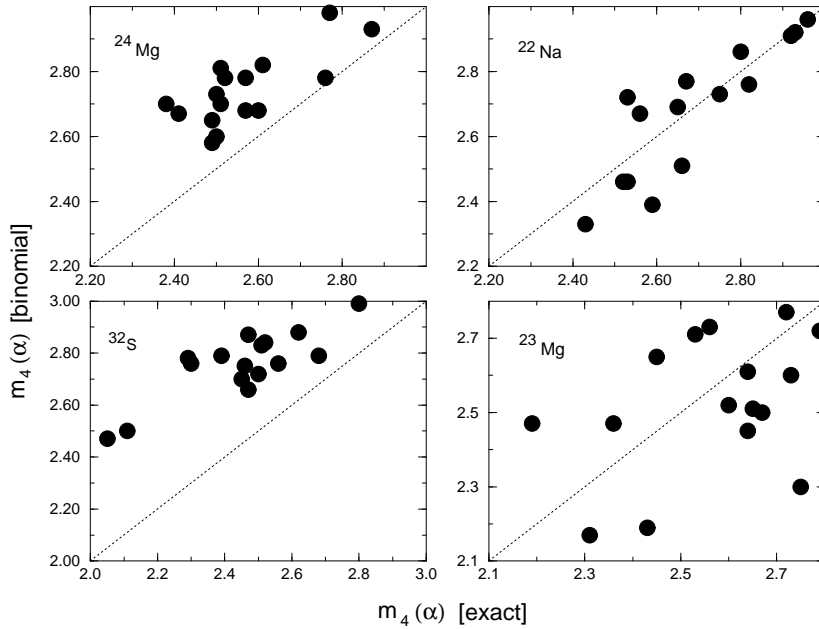


FIG. 6. Comparison of the low-lying exact (configuration) scaled fourth moments $m_4(\alpha)$ with those calculated from the standard binomial. The dotted line is to guide the eye.